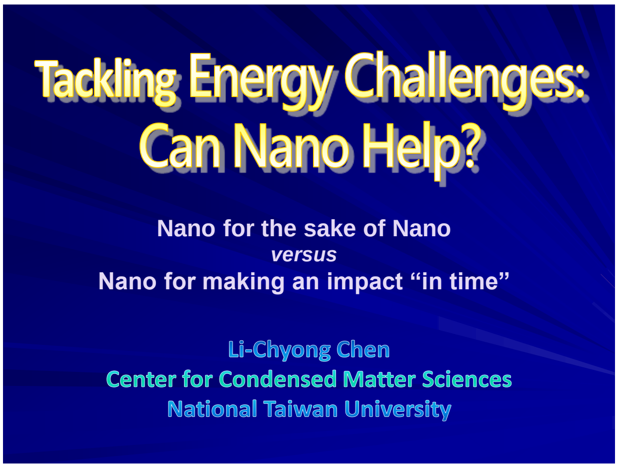
Tackling Energy Challenges: Can Nano Help?
Nano for the sake of Nano
versus
Nano for making an impact "in time"
Li-Chyong Chen
Center for Condensed Matter Sciences
National Taiwan University


Motivation
Green & Miniaturized Products
Nano-materials for Energy Applications
Li-ion Battery
Super Capacitor
Solar Cell
Bio – Fuel Cell
Fuel Cell

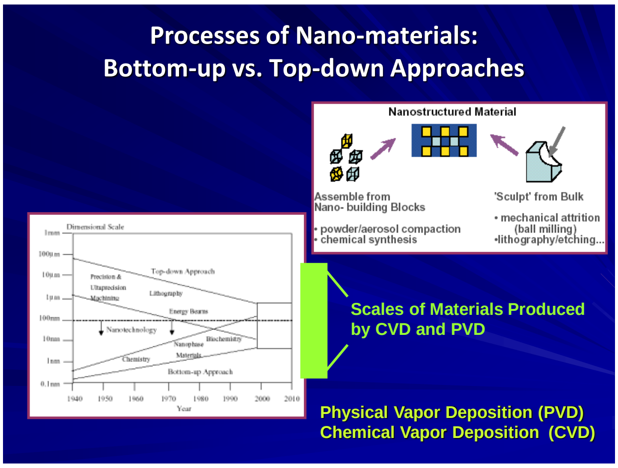
Processes of Nano-materials:
Bottom-up vs. Top-down Approaches
Nanostructured Material
Assemble from Nano- building Blocks
• powder/aerosol compaction
• chemical synthesis
'Sculpt' from Bulk
• mechanical attrition (ball milling)
•lithography/etching...
Dimensional Scale
Top-down Approach
Bottom-up Approach
Year
Scales of Materials Produced by CVD and PVD
Physical Vapor Deposition (PVD)
Chemical Vapor Deposition (CVD)

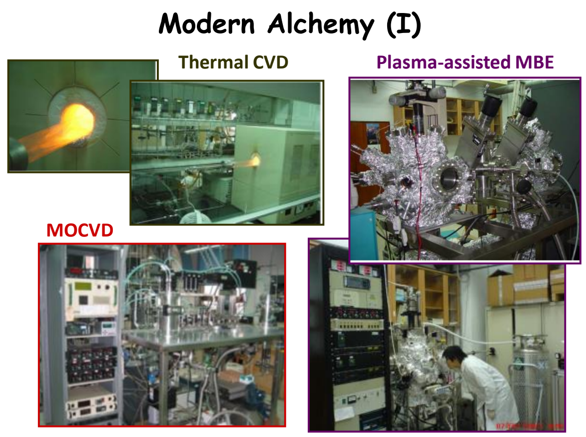
Modern Alchemy (I)
Thermal CVD
Plasma-assisted MBE
MOCVD

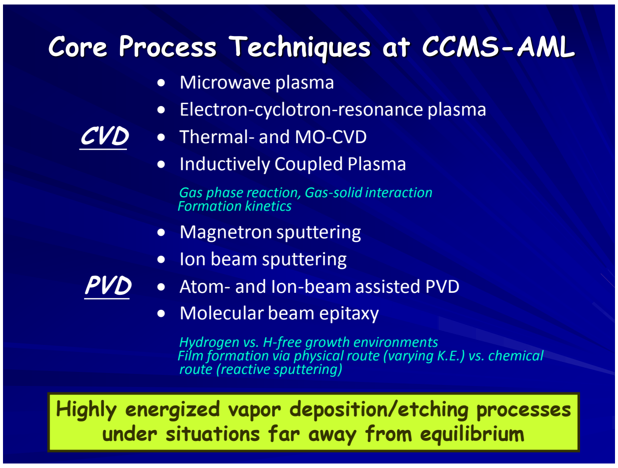
Core Process Techniques at CCMS-AML
CVD
• Microwave plasma
• Electron-cyclotron-resonance plasma
• Thermal- and MO-CVD
• Inductively Coupled Plasma
Gas phase reaction, Gas-solid interaction
Formation kinetics
PVD
• Magnetron sputtering
• Ion beam sputtering
• Atom- and Ion-beam assisted PVD
• Molecular beam epitaxy
Hydrogen vs. H-free growth environments
Film formation via physical route (varying K.E.) vs. chemical route (reactive sputtering)
Highly energized vapor deposition/etching processes under situations far away from equilibrium

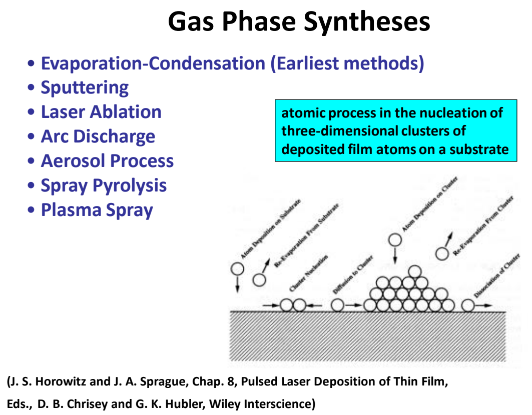
Gas Phase Syntheses
• Evaporation-Condensation (Earliest methods)
• Sputtering
• Laser Ablation
• Arc Discharge
• Aerosol Process
• Spray Pyrolysis
• Plasma Spray
atomic process in the nucleation of three-dimensional clusters of deposited film atoms on a substrate
(J. S. Horowitz and J. A. Sprague, Chap. 8, Pulsed Laser Deposition of Thin Film, Eds., D. B. Chrisey and G. K. Hubler, Wiley Interscience)

Gas Phase Pressure and Mean Free Path

- $P = 1/3 nMv^2/N_A$

Where N_A is Avogadro's number, v^2 is mean square velocity, M the molecular weight and n is the number of molecules per unit volume.

- $\lambda_{mpf} = 5 \times 10^{-3}/P$

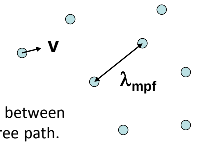

The mean distance traveled by molecules between successive collisions is called the mean-free path.

Strong Function of Kinetic Energy or Temperature

Correlation between Gas Pressure and Other Film Formation Parameters

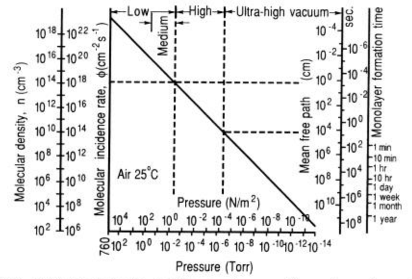

Figure 2-2. Molecular density, incidence rate, mean-free path, and monolayer formation time as a function of pressure. (Reprinted with permission from Ref. 2).

(A. Roth, Vacuum Technology, 1976)

Size Control of Clusters and Nanoparticles

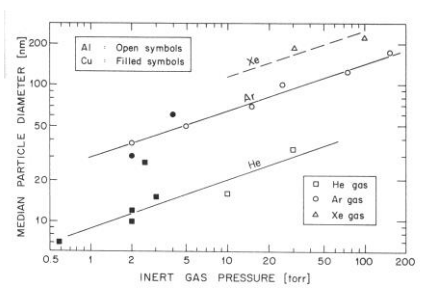

(C. G. Granqvist and R. A. Buhrman, JAP, 1976)

Structural Zones in Physical Processes: Fully-developed Grain Structures

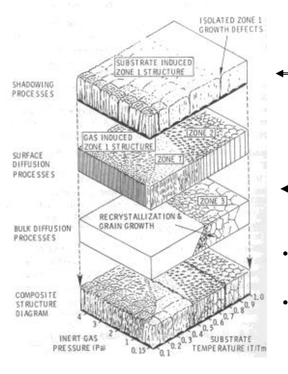

Geometric constrain
- **roughness of surface**
- **line-of-sight impingement**

Atomistic processes
- **surface diffusion**
- **bulk diffusion**
- **desorption**

- **Movchan and Demchishin, Phys. Met. Metallogr. 1969 (zone 1, 2, 3)**
- **J.A. Thornton, Ann. Rev. Mater. Sci., 1977 (zone T)**

Ion-Surface Interaction

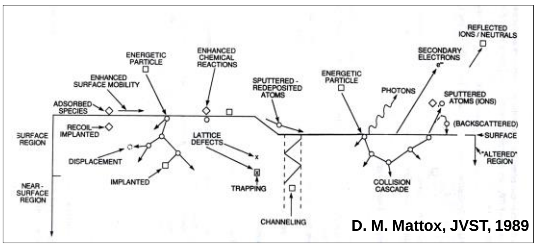

D. M. Mattox, JVST, 1989

Applications: deposition, surface modification, implantation, etc.

Schematic of Chemical Vapor Deposition

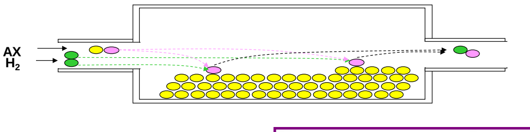

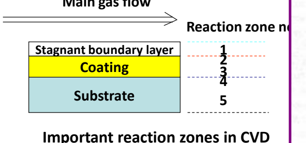

Important reaction zones in CVD

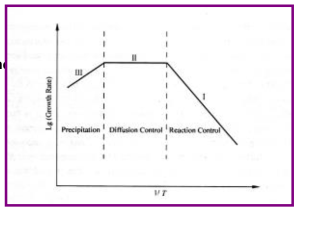

Common CVD Precursors

Properties of common organometallic precursors for semiconductor growth.

Element	OM source	Symbol	Vapor pressure at 25°C (Torr)	Vapor pressure equation [137] $\log P = B - A/T$		Comments
				A	B	
Gallium	Trimethylgallium	TMGa, TMG	228.2	1703	8.07	Most common Ga source, source of C in CBE
	Triethylgallium	TEG, TEGa	5.9	2222	8.224	Best source for high-purity source, low growth rates
Aluminum	Trimethylaluminum	TMA	11.6	2134.8	8.224	Most common aluminum source, high carbon incorporation
	Triethylaluminum	TEA	0.03	2361.2[a]	8.999	Very low vapor pressure, reduced C incorporation, parasitic reactions
	Tri-isobutyl aluminum	TIBA	0.15	1710.3[b]	7.121	Source for Al metal as well as Al alloys, possibly reduced C incorporation, unstable
	Trimethylamine alane	TMAA				Promising source for high-purity Al-containing materials, low vapor pressure
Indium	Trimethylindium	TMI	2.58	3014	10.52	Most common indium source, source stability and reproducibility problems, solid
	Triethylindium	TEI	0.31	2815	8.93	Liquid indium source, low vapor pressure, pre-reaction problems
	Ethyldimethylindium	EDMIn	3.2			Promising alternative to TMIn, liquid, may not be thermally stable
Arsenic	Tertiarybutyl arsine	TBA, TBAs	182.1	1562.3	7.5	Liquid alternative to arsine, high-quality material, very expensive
	Diethyl arsine	DEAs	50.6	1680	7.339	Liquid alternative to arsine, good-quality material, very expensive
	Trimethylarsine	TMAs	275	1480	7.405	Poor alternative to arsine due to carbon incorporation, used as carbon doping source
Phosphorus	Tertiarybutyl phosphine	TBP	265.7	1539	7.586	Best liquid alternative to phosphine
Antimony	Trimethyl antimony	TMSb	103.6	1697	7.707	Relatively high decomposition temperature
Zinc	Diethylzinc	DEZ, DEZn	16.1	2109	8.28	Zn doping source, also source for II–VI compounds
	Dimethylzinc	DMZ, DMZn	365	1560	7.802	Zn doping source, very high vapor pressure, source for II–VI compounds
	DEZn–amine	DMZA				Promising source for II–VI materials, resistant to pre-reaction with hydrides
Iron	Iron pentacarbonyl		35			Source for semi-insulating InP

[a] $\log P = B - A/(T - 73.82)$.
[b] $\log P = B - A/(T - 83.92)$.

Plasma-assisted CVD

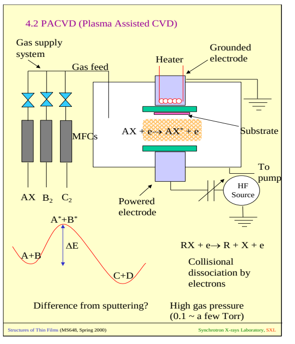

- Generation of plasma: DC, RF, Microwave, ECR
- Typical kinetic energy of electron ~ 1-10 eV, and ion ~ 0.02-0.1 eV
- Reduced activation energy

Nucleation and Growth of Films: The Three Conventional Modes

2-d full-monolayer
Frank-van der Merwe

3-d (or "0-d") island
Volmer-Weber

2-d and 3-d
Stranski-Krastinov

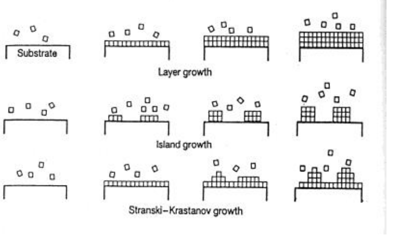

Selection of Growth Modes

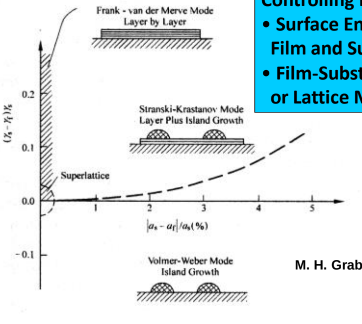

Controlling Parameters:
- Surface Energies of both Film and Substrate
- Film-Substrate Interface Energy or Lattice Mismatch

M. H. Grabow, et al, TMS, 1986.

Vapor-Liquid-Solid Growth

Alloying ⟹ Nucleation ⟹ Growth

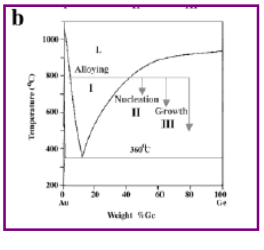

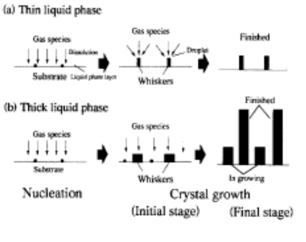

Y. Wu and P. Yang, *J. Am. Chem. Soc.* 2001

Introducing Catalyst *via* Different Pathways: Gaseous Source *versus* Solid/Liquid Source

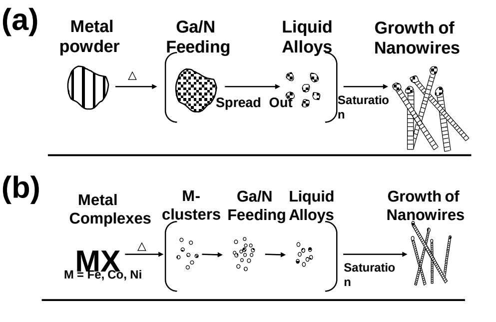

C.-C. Chen *et al.*, *J. Am. Chem. Soc.*, 2001

Growth of CNT with Catalyst

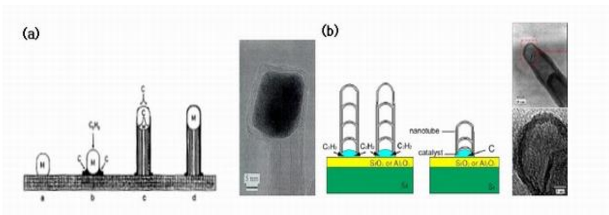

Fig. 8 Growth model of carbon nanotube by chemical vapor deposition

(a) Tip growth model [20] (b) Base growth model [49]

C. H. Bartholomew

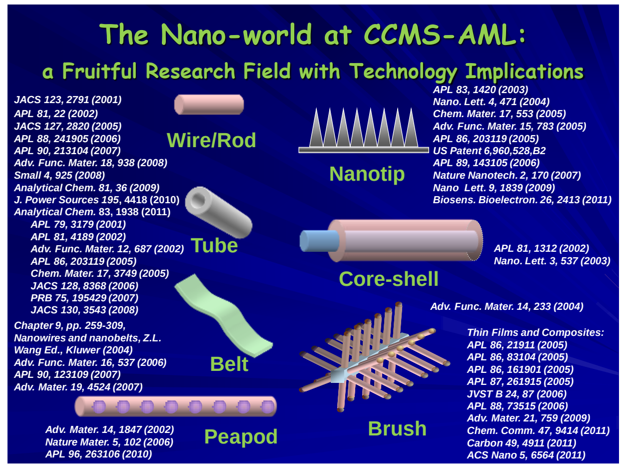

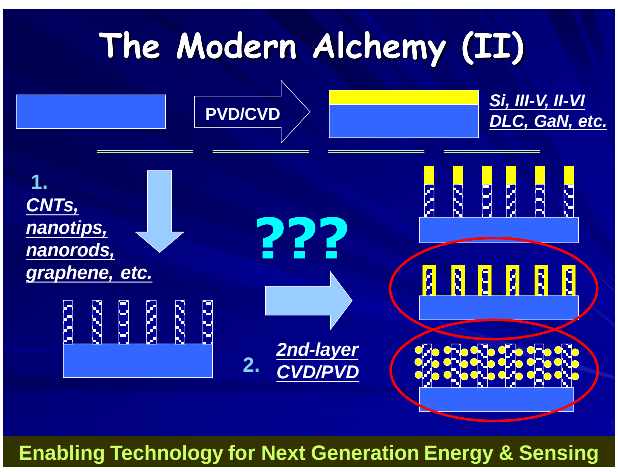

Arrayed Graphene and Carbon Nanotubes: On-chip Synthesis, Electrochemical Properties for Energy and Sensing Applications

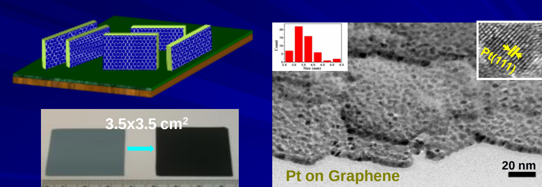

Outline

- Quest of next-generation energy solution
  - Why graphene and CNT? How they can help?
- On-chip, direct-growth of graphene and CNT
  - Evidence of strain in few-layer graphene
  - Deposition of Pt on graphene and CNT
- Electrochemical properties
  - Charge transfer between Pt and graphene
- Supercapacitor and fuel cell
- *Others: sensor, transparent conduction film*

CNTs or Graphene for Energy Applications

- **Green and miniaturized products**:
  - power for portable electronics
- **Integrated material/device design**:
  - enhanced electrochemical properties
  - novel micro energy devices

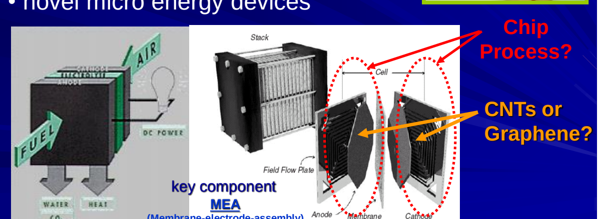

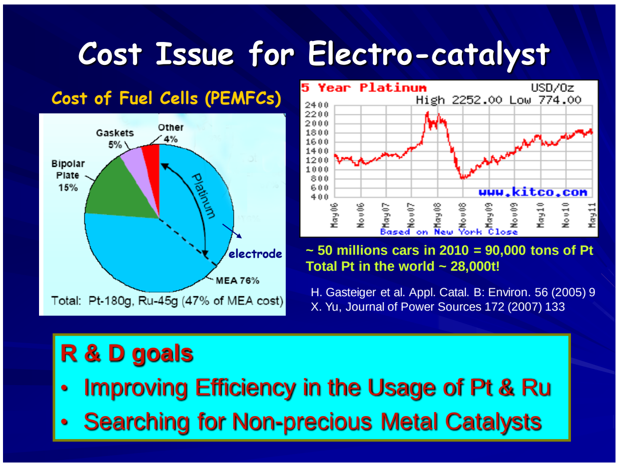
Cost Issue for Electro-catalyst
Cost of Fuel Cells (PEMFCs)
Gaskets 5%
Other 4%
Bipolar Plate 15%
Platinum
electrode
MEA 76%
Total: Pt-180g, Ru-45g (47% of MEA cost)
5 Year Platinum USD/Oz
High 2252.00 Low 774.00
www.kitco.com
~ 50 millions cars in 2010 = 90,000 tons of Pt
Total Pt in the world ~ 28,000t!
H. Gasteiger et al. Appl. Catal. B: Environ. 56 (2005) 9
X. Yu, Journal of Power Sources 172 (2007) 133
R & D goals
• Improving Efficiency in the Usage of Pt & Ru
• Searching for Non-precious Metal Catalysts

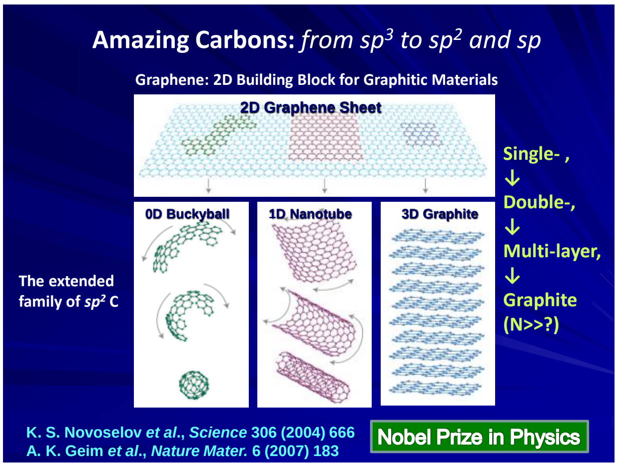
Amazing Carbons: from sp3 to sp2 and sp
Graphene: 2D Building Block for Graphitic Materials
2D Graphene Sheet
0D Buckyball
1D Nanotube
3D Graphite
The extended family of sp2 C
Single- ,
Double-,
Multi-layer,
Graphite (N>>?)
K. S. Novoselov et al., Science 306 (2004) 666
A. K. Geim et al., Nature Mater. 6 (2007) 183
Nobel Prize in Physics

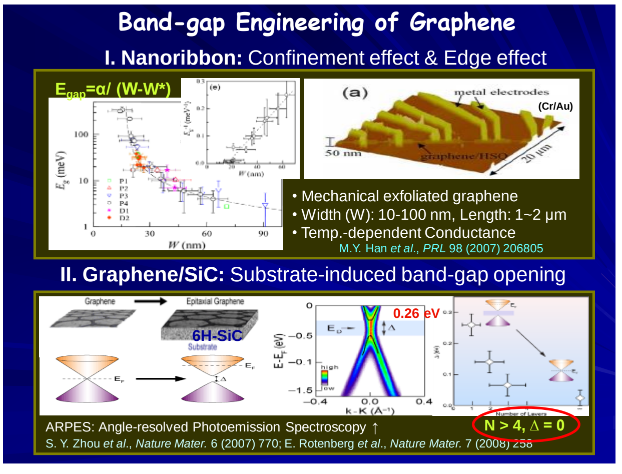
Band-gap Engineering of Graphene
I. Nanoribbon: Confinement effect & Edge effect
Egap=α/ (W-W*)
metal electrodes (Cr/Au)
graphene/HSQ
• Mechanical exfoliated graphene
• Width (W): 10-100 nm, Length: 1~2 μm
• Temp.-dependent Conductance
M.Y. Han et al., PRL 98 (2007) 206805
II. Graphene/SiC: Substrate-induced band-gap opening
6H-SiC
0.26 eV
N > 4, Δ = 0
ARPES: Angle-resolved Photoemission Spectroscopy
S. Y. Zhou et al., Nature Mater. 6 (2007) 770; E. Rotenberg et al., Nature Mater. 7 (2008) 258

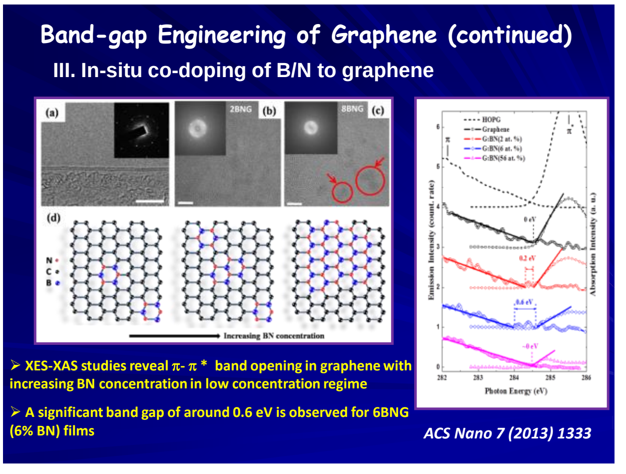
Band-gap Engineering of Graphene (continued)
III. In-situ co-doping of B/N to graphene
Increasing BN concentration
➢ XES-XAS studies reveal π- π* band opening in graphene with increasing BN concentration in low concentration regime
➢ A significant band gap of around 0.6 eV is observed for 6BNG (6% BN) films
ACS Nano 7 (2013) 1333

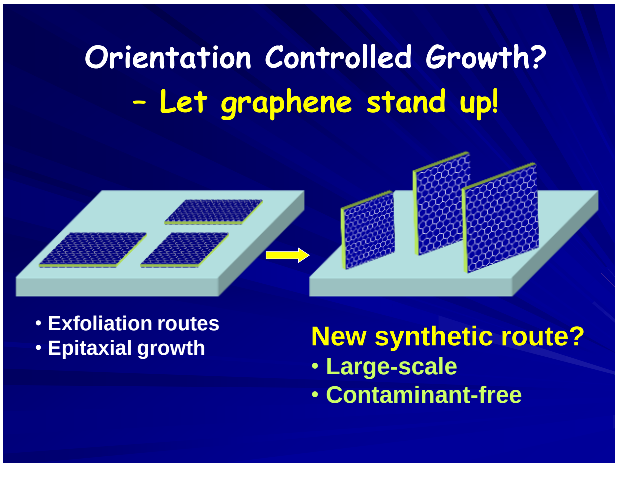
Orientation Controlled Growth?
- Let graphene stand up!
• Exfoliation routes
• Epitaxial growth
New synthetic route?
• Large-scale
• Contaminant-free

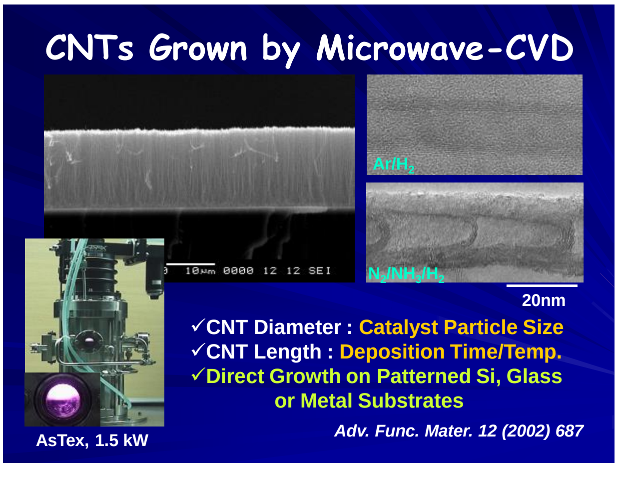
CNTs Grown by Microwave-CVD
Ar/H2
N2/NH3/H2
20nm
AsTex, 1.5 kW
✓CNT Diameter : Catalyst Particle Size
✓CNT Length : Deposition Time/Temp.
✓Direct Growth on Patterned Si, Glass or Metal Substrates
Adv. Func. Mater. 12 (2002) 687

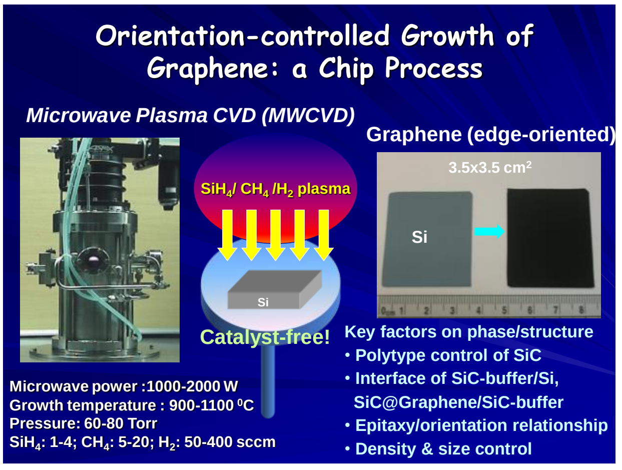
Orientation-controlled Growth of Graphene: a Chip Process
Microwave Plasma CVD (MWCVD)
Graphene (edge-oriented)
SiH_4/ CH_4 /H_2 plasma
3.5x3.5 cm²
Si
Si
Catalyst-free!
Key factors on phase/structure
• Polytype control of SiC
• Interface of SiC-buffer/Si, SiC@Graphene/SiC-buffer
• Epitaxy/orientation relationship
• Density & size control
Microwave power :1000-2000 W
Growth temperature : 900-1100 °C
Pressure: 60-80 Torr
SiH_4: 1-4; CH_4: 5-20; H_2: 50-400 sccm

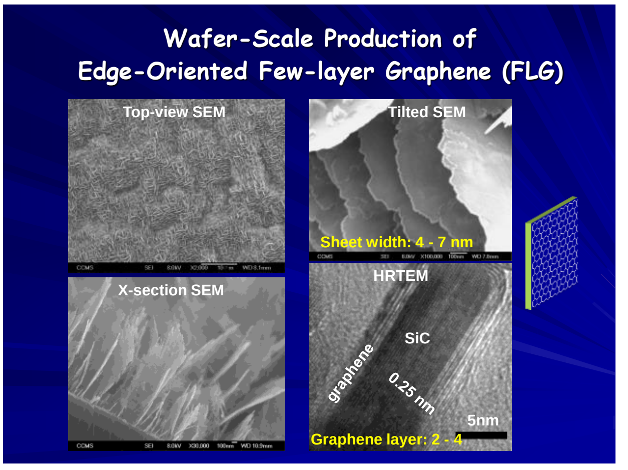
Wafer-Scale Production of Edge-Oriented Few-layer Graphene (FLG)
Top-view SEM
Tilted SEM
Sheet width: 4 - 7 nm
X-section SEM
HRTEM
SiC
graphene
0.25 nm
5nm
Graphene layer: 2 - 4

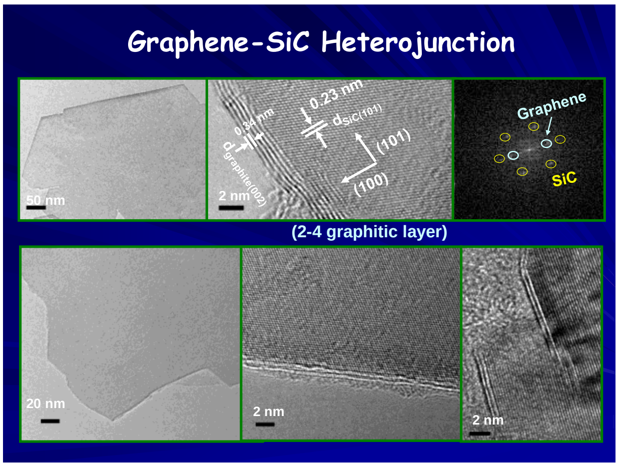
Graphene-SiC Heterojunction
50 nm
0.23 nm
$d_{SiC(101)}$
(101)
(100)
2 nm
Graphene
SiC
(2-4 graphitic layer)
20 nm
2 nm
2 nm

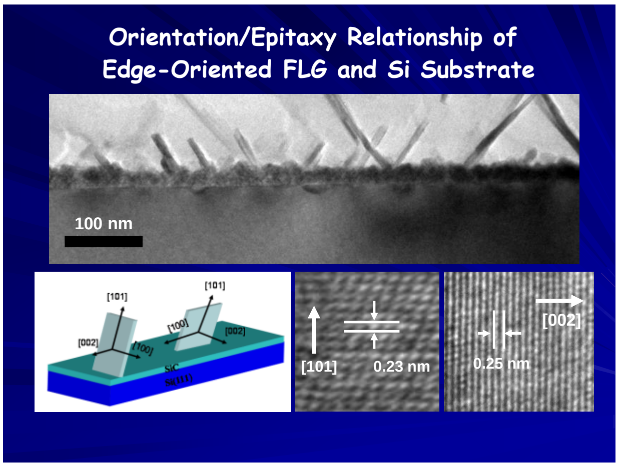
Orientation/Epitaxy Relationship of Edge-Oriented FLG and Si Substrate
100 nm
[101]
[101]
[002]
[100]
[002]
[101]
0.23 nm
0.25 nm
[002]

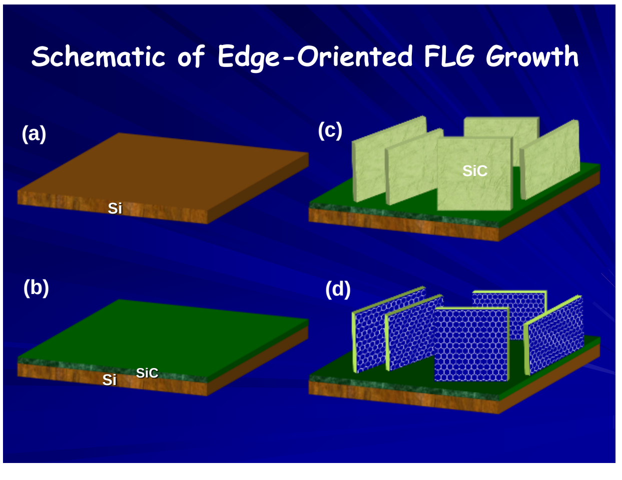
Schematic of Edge-Oriented FLG Growth
(a)
Si
(b)
Si
SiC
(c)
SiC
(d)

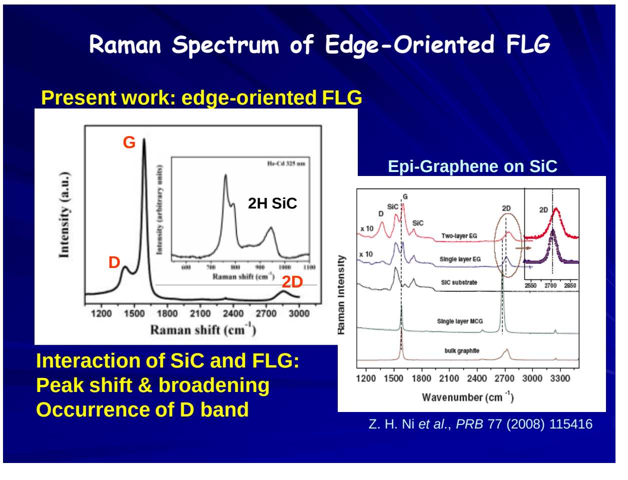
Raman Spectrum of Edge-Oriented FLG
Present work: edge-oriented FLG
G
D
2D
2H SiC
Intensity (a.u.)
Raman shift (cm⁻¹)
Epi-Graphene on SiC
Raman Intensity
Wavenumber (cm⁻¹)
Interaction of SiC and FLG:
Peak shift & broadening
Occurrence of D band
Z. H. Ni et al., PRB 77 (2008) 115416

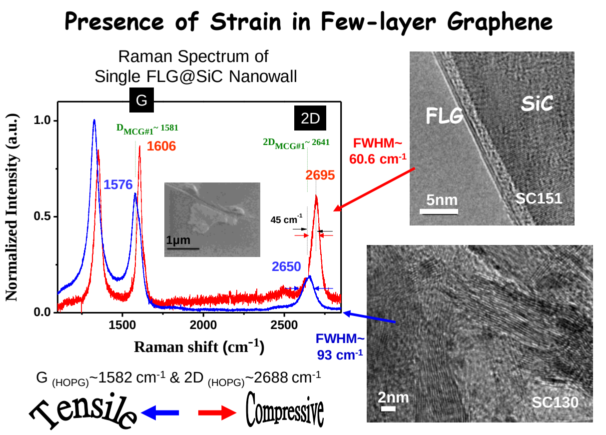
Presence of Strain in Few-layer Graphene
Raman Spectrum of Single FLG@SiC Nanowall
G
2D
1606
1576
2695
2650
45 cm-1
1μm
FWHM~ 60.6 cm-1
FWHM~ 93 cm-1
Normalized Intensity (a.u.)
Raman shift (cm-1)
FLG
SiC
5nm
SC151
2nm
SC130
G (HOPG)~1582 cm-1 & 2D (HOPG)~2688 cm-1
Tensile
Compressive

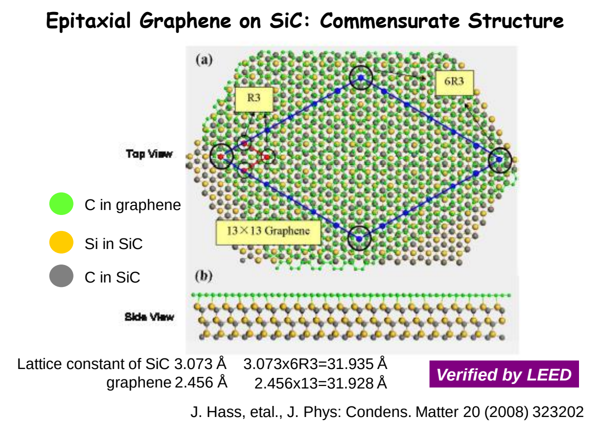
Epitaxial Graphene on SiC: Commensurate Structure
(a)
Top View
R3
6R3
13×13 Graphene
(b)
Side View
C in graphene
Si in SiC
C in SiC
Lattice constant of SiC 3.073 Å 3.073x6R3=31.935 Å
graphene 2.456 Å 2.456x13=31.928 Å
Verified by LEED
J. Hass, etal., J. Phys: Condens. Matter 20 (2008) 323202

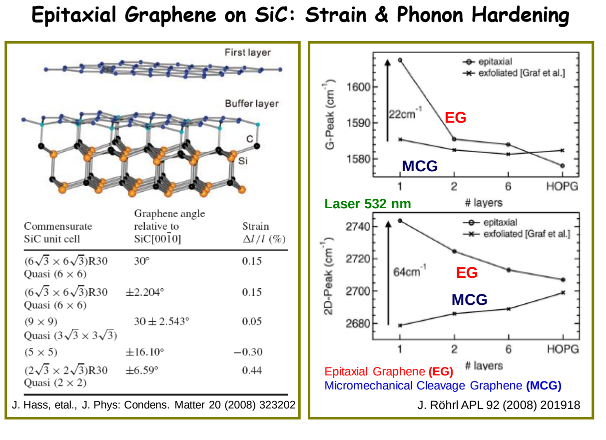
Epitaxial Graphene on SiC: Strain & Phonon Hardening
First layer
Buffer layer
C
Si
Commensurate SiC unit cell | Graphene angle relative to SiC[0010] | Strain Δl/l (%)
(6√3 × 6√3)R30 Quasi (6 × 6) | 30° | 0.15
(6√3 × 6√3)R30 Quasi (6 × 6) | ±2.204° | 0.15
(9 × 9) Quasi (3√3 × 3√3) | 30 ± 2.543° | 0.05
(5 × 5) | ±16.10° | −0.30
(2√3 × 2√3)R30 Quasi (2 × 2) | ±6.59° | 0.44
J. Hass, etal., J. Phys: Condens. Matter 20 (2008) 323202
epitaxial
exfoliated [Graf et al.]
G-Peak (cm-1)
22cm-1
EG
MCG
layers
Laser 532 nm
2D-Peak (cm-1)
64cm-1
HOPG
Epitaxial Graphene (EG)
Micromechanical Cleavage Graphene (MCG)
J. Röhrl APL 92 (2008) 201918

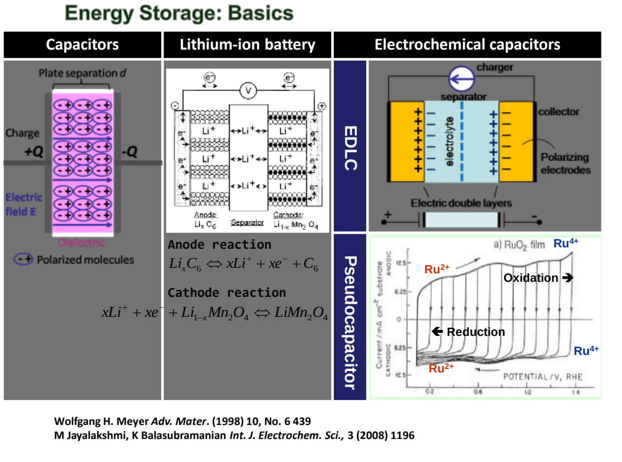
Energy Storage: Basics
Capacitors
Lithium-ion battery
Electrochemical capacitors
Plate separation d
Charge +Q
-Q
Electric field E
Dielectric
Polarized molecules
Anode reaction
$Li_xC_6 \Leftrightarrow xLi^+ + xe^- + C_6$
Cathode reaction
$xLi^+ + xe^- + Li_{1-x}Mn_2O_4 \Leftrightarrow LiMn_2O_4$
EDLC
charger
separator
collector
electrolyte
Polarizing electrodes
Electric double layers
Pseudocapacitor
a) RuO2 film
Ru4+
Ru2+
Oxidation
Reduction
POTENTIAL / V, RHE
Wolfgang H. Meyer Adv. Mater. (1998) 10, No. 6 439
M Jayalakshmi, K Balasubramanian Int. J. Electrochem. Sci., 3 (2008) 1196

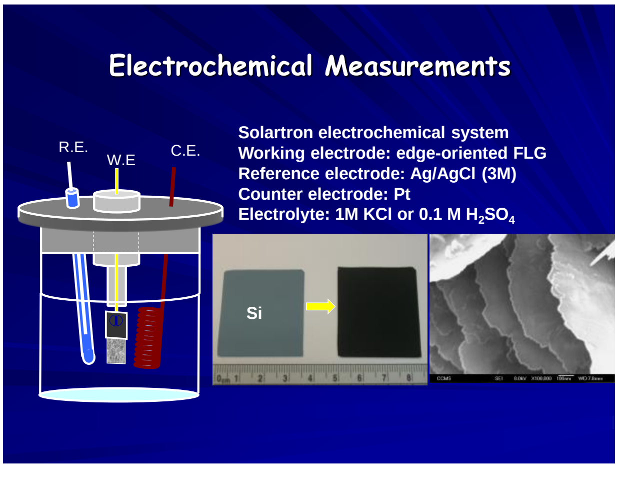
Electrochemical Measurements
R.E.
W.E
C.E.
Solartron electrochemical system
Working electrode: edge-oriented FLG
Reference electrode: Ag/AgCl (3M)
Counter electrode: Pt
Electrolyte: 1M KCl or 0.1 M H2SO4
Si

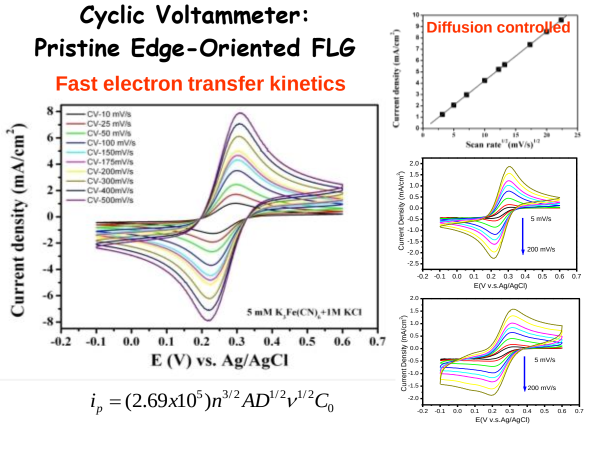
Cyclic Voltammeter:
Pristine Edge-Oriented FLG
Fast electron transfer kinetics
Diffusion controlled
Current density (mA/cm2)
E (V) vs. Ag/AgCl
5 mM K3Fe(CN)6+1M KCl
CV-10 mV/s
CV-25 mV/s
CV-50 mV/s
CV-100 mV/s
CV-150mV/s
CV-175mV/s
CV-200mV/s
CV-300mV/s
CV-400mV/s
CV-500mV/s
5 mV/s
200 mV/s
$i_p = (2.69x10^5)n^{3/2}AD^{1/2}v^{1/2}C_0$

Nearly Ideal Electron Transfer Kinetics

CV of edge-oriented FLG: Nerstian Behavior
One-electron Transfer & Reversible Process

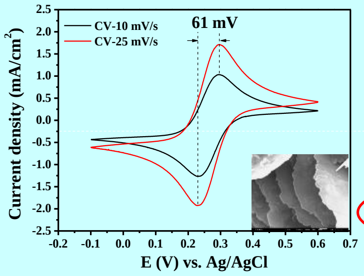

Electrode	ΔE_p (mV)
Pt	88
CNTs	59
Basal plane HOPG	>700
Edge plane HOPG	70
Edge-oriented FLG (our work)	61

HOPG (highly ordered pyrolytic graphite)
J.M. Nugent *et al.*, *Nano Lett.* 1 (2001) 87

Capacitive Properties
(Double-layer, non-Faradaic)

Cyclic Voltammograms in 1M H_2SO_4 Solution

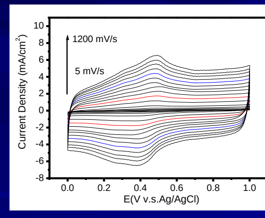

Capacitance–Voltage Curves

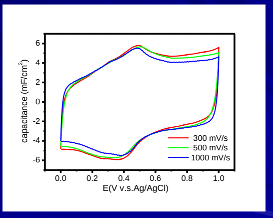

- Scan rate can be up to 1200 mV/s.
- With aqueous-based supercapacitors, it is generally limited to around 1V, due to water electrolysis.

Galvanostatic Charge/Discharge Analyses

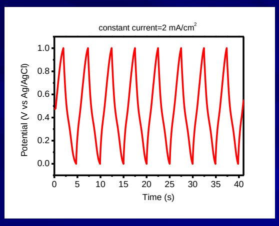

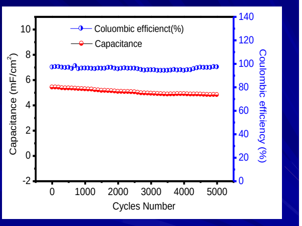

$$Cp = \frac{I}{a(dV/dt)} = 5.15\, mF/cm^2$$

$$\frac{C_{discharge}}{C_{charge}} = Coulombic\ efficiency\ (\%)$$

Electrolyte: 1 M H_2SO_4 solution
Potential = 0.0 V ~ 1.0 V
Constant current = 2.0 mA/cm²

Edge-oriented FLG-array vs. Planar FLG

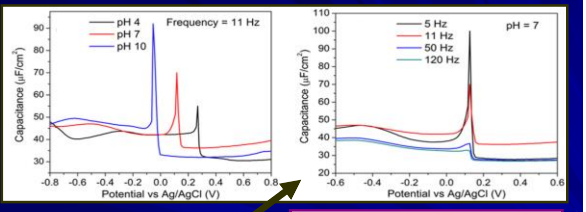

30-fold Increase in Peak Capacitance!
Edge-oriented FLG: 100μF/cm² (5Hz)

Planar-FLG: 3μF/cm² (5Hz)

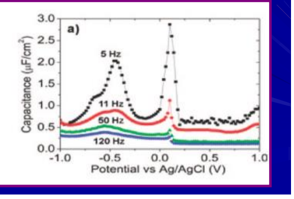

Graphene (or CNT)-Pt Composite as Electro-Catalyst for Fuel Cell

Membrane Electrode Assembly in DMFC

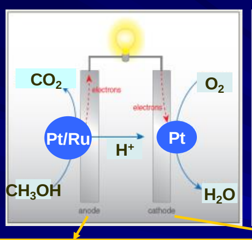

$CH_3OH + {}^3/_2O_2 \rightarrow CO_2 + 2H_2O$, E_{ocv}: 1.21

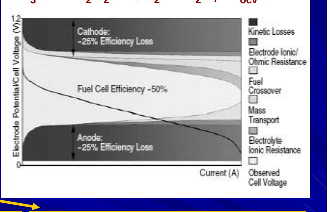

Anode Challenges:
- Poor catalytic kinetics
- Catalyst poisoned
- Catalyst agglomerated
- Catalyst inactive (Ru → RuO_x)
- CO_2 stuck

Cathode Challenges:
- Poor catalytic kinetics
- Catalyst agglomerated
- Methanol crossover
- Flooding
- Support corrosion

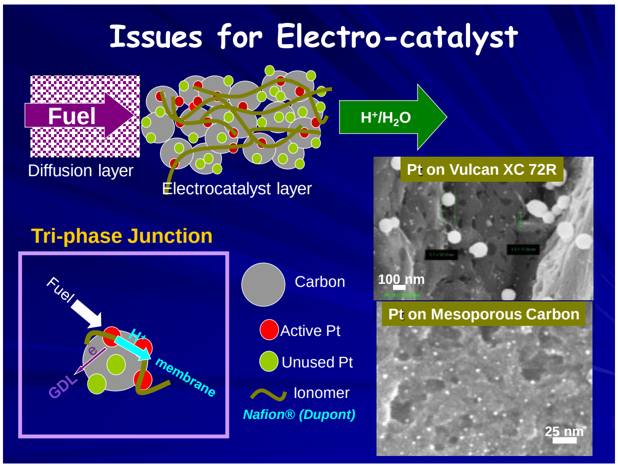
Issues for Electro-catalyst
Fuel
Diffusion layer
Electrocatalyst layer
H+/H2O
Pt on Vulcan XC 72R
100 nm
Tri-phase Junction
Fuel
H+
membrane
GDL
e
Carbon
Active Pt
Unused Pt
Ionomer
Nafion® (Dupont)
Pt on Mesoporous Carbon
25 nm

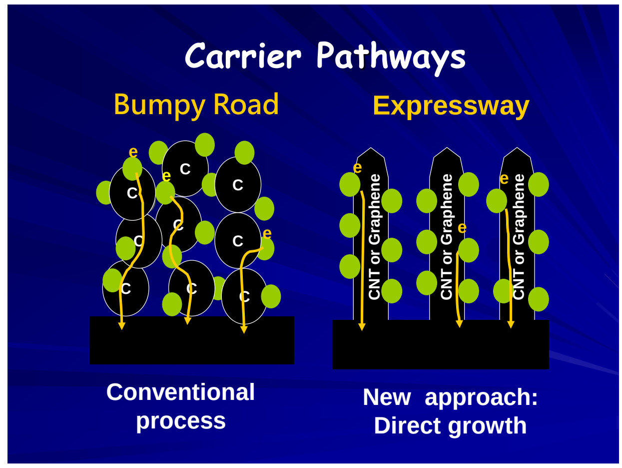
Carrier Pathways
Bumpy Road
Expressway
CNT or Graphene
Conventional process
New approach: Direct growth

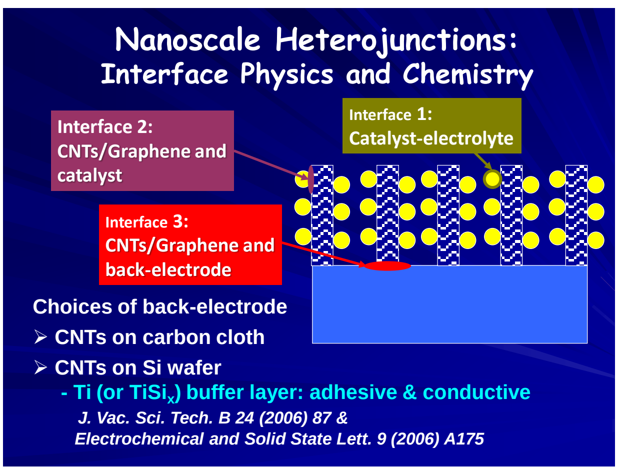
Nanoscale Heterojunctions: Interface Physics and Chemistry
Interface 2: CNTs/Graphene and catalyst
Interface 1: Catalyst-electrolyte
Interface 3: CNTs/Graphene and back-electrode
Choices of back-electrode
➢ CNTs on carbon cloth
➢ CNTs on Si wafer
- Ti (or TiSix) buffer layer: adhesive & conductive
J. Vac. Sci. Tech. B 24 (2006) 87 &
Electrochemical and Solid State Lett. 9 (2006) A175

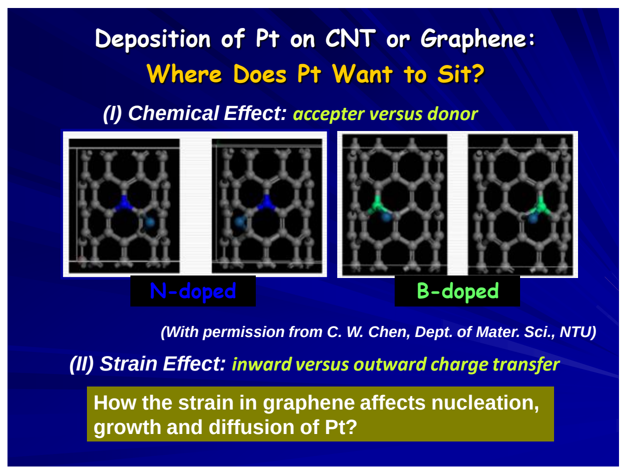
Deposition of Pt on CNT or Graphene:
Where Does Pt Want to Sit?
(I) Chemical Effect: accepter versus donor
N-doped
B-doped
(With permission from C. W. Chen, Dept. of Mater. Sci., NTU)
(II) Strain Effect: inward versus outward charge transfer
How the strain in graphene affects nucleation, growth and diffusion of Pt?

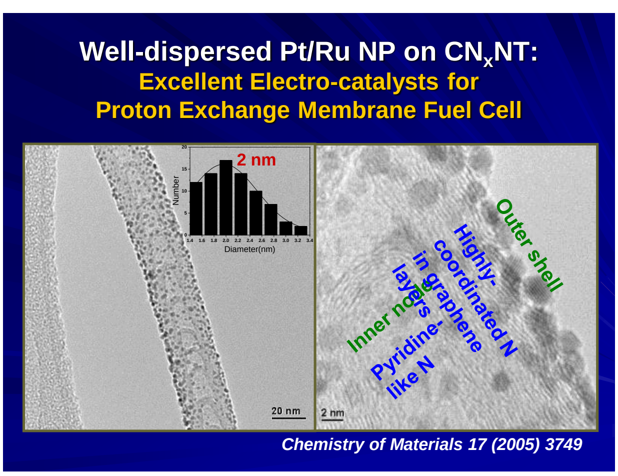
Well-dispersed Pt/Ru NP on CNxNT:
Excellent Electro-catalysts for
Proton Exchange Membrane Fuel Cell
2 nm
Number
Diameter(nm)
20 nm
Outer shell
Highly-coordinated N
in graphene layers
Inner nodes
Pyridine-like N
2 nm
Chemistry of Materials 17 (2005) 3749

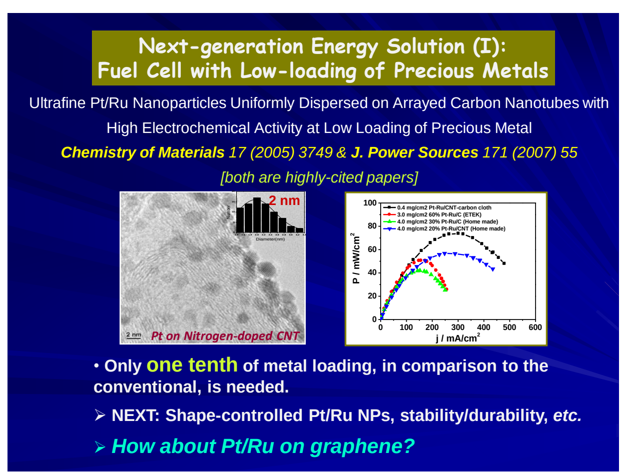
Next-generation Energy Solution (I):
Fuel Cell with Low-loading of Precious Metals
Ultrafine Pt/Ru Nanoparticles Uniformly Dispersed on Arrayed Carbon Nanotubes with High Electrochemical Activity at Low Loading of Precious Metal
Chemistry of Materials 17 (2005) 3749 & J. Power Sources 171 (2007) 55
[both are highly-cited papers]
2 nm
Pt on Nitrogen-doped CNT
P / mW/cm2
j / mA/cm2
• Only one tenth of metal loading, in comparison to the conventional, is needed.
➢ NEXT: Shape-controlled Pt/Ru NPs, stability/durability, etc.
➢ How about Pt/Ru on graphene?

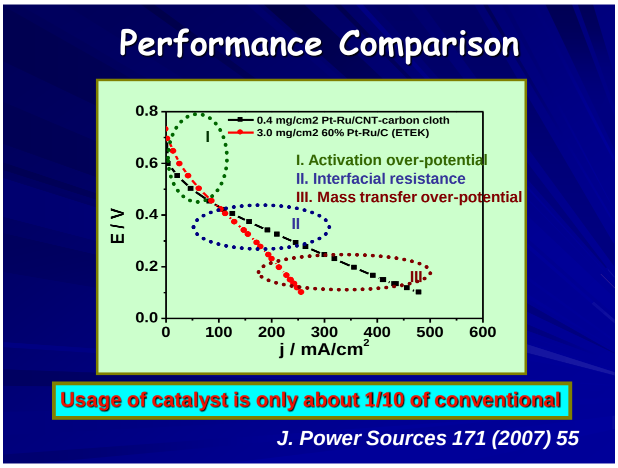
Performance Comparison
0.4 mg/cm2 Pt-Ru/CNT-carbon cloth
3.0 mg/cm2 60% Pt-Ru/C (ETEK)
I. Activation over-potential
II. Interfacial resistance
III. Mass transfer over-potential
E / V
j / mA/cm2
Usage of catalyst is only about 1/10 of conventional
J. Power Sources 171 (2007) 55

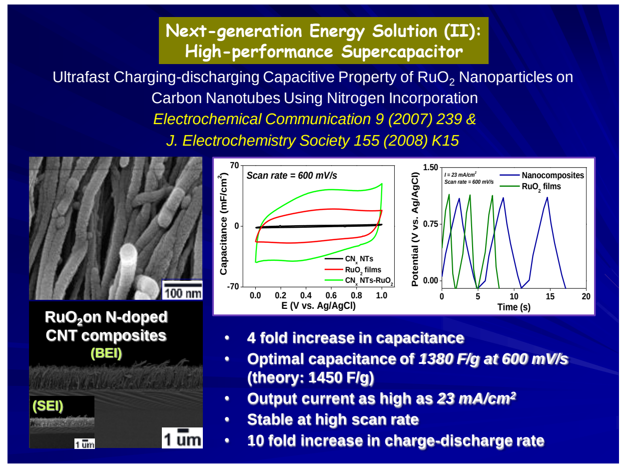
Next-generation Energy Solution (II):
High-performance Supercapacitor
Ultrafast Charging-discharging Capacitive Property of RuO2 Nanoparticles on Carbon Nanotubes Using Nitrogen Incorporation
Electrochemical Communication 9 (2007) 239 &
J. Electrochemistry Society 155 (2008) K15
RuO2 on N-doped CNT composites
(BEI)
(SEI)
100 nm
1 um
Scan rate = 600 mV/s
Capacitance (mF/cm2)
E (V vs. Ag/AgCl)
Potential (V vs. Ag/AgCl)
Time (s)
Nanocomposites
RuO2 films
4 fold increase in capacitance
Optimal capacitance of 1380 F/g at 600 mV/s (theory: 1450 F/g)
Output current as high as 23 mA/cm2
Stable at high scan rate
10 fold increase in charge-discharge rate

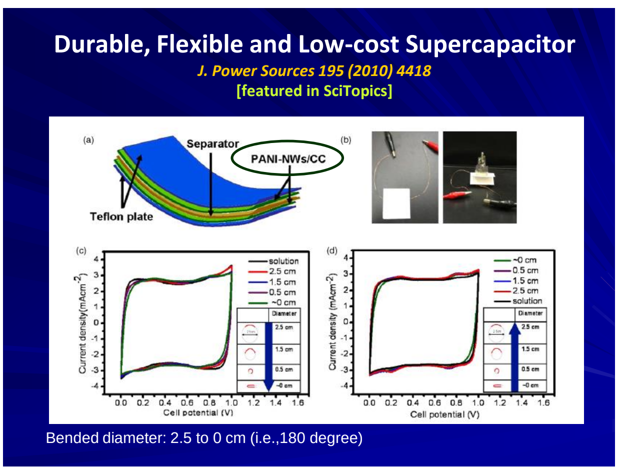
Durable, Flexible and Low-cost Supercapacitor
J. Power Sources 195 (2010) 4418
[featured in SciTopics]
Separator
PANI-NWs/CC
Teflon plate
Current density (mAcm-2)
Cell potential (V)
Bended diameter: 2.5 to 0 cm (i.e.,180 degree)

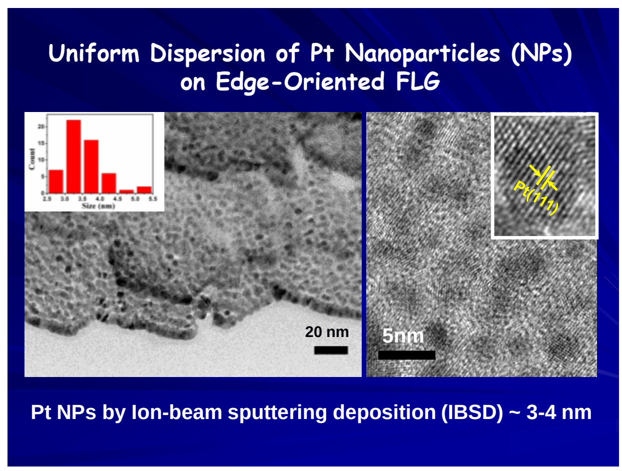
Uniform Dispersion of Pt Nanoparticles (NPs)
on Edge-Oriented FLG
20 nm
5nm
Pt(111)
Pt NPs by Ion-beam sputtering deposition (IBSD) ~ 3-4 nm

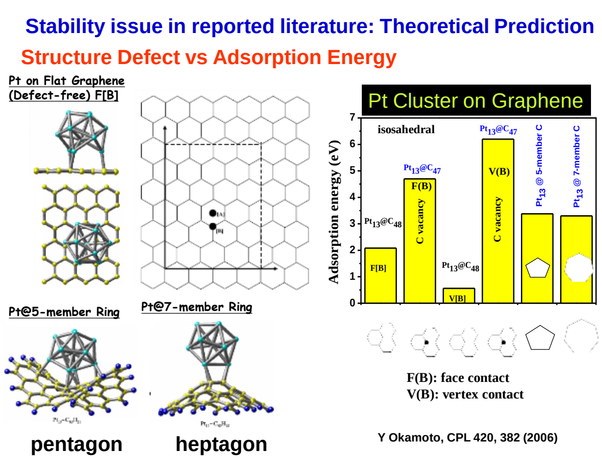
Stability issue in reported literature: Theoretical Prediction
Structure Defect vs Adsorption Energy
Pt on Flat Graphene
(Defect-free) F[B]
Pt@5-member Ring
Pt@7-member Ring
pentagon
heptagon
Pt Cluster on Graphene
isosahedral
Adsorption energy (eV)
C vacancy
F(B): face contact
V(B): vertex contact
Y Okamoto, CPL 420, 382 (2006)

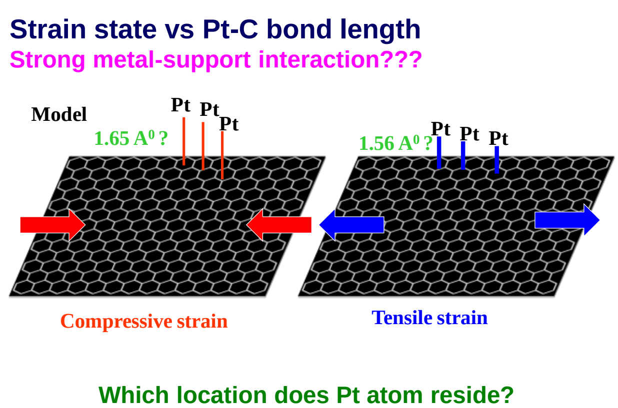
Strain state vs Pt-C bond length
Strong metal-support interaction???
Model
Pt
1.65 A0 ?
1.56 A0 ?
Compressive strain
Tensile strain
Which location does Pt atom reside?

Determination of N Incorporation Site

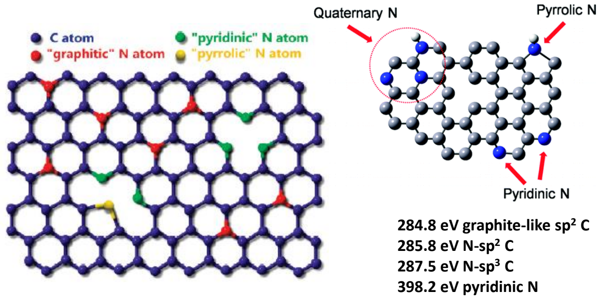

284.8 eV graphite-like sp² C
285.8 eV N-sp² C
287.5 eV N-sp³ C
398.2 eV pyridinic N
400.1 eV pyrrolic N
401.7 eV substitutional N

Pyridinic N (six-member ring) 398.2 eV
Pyrrolic N (five-member ring) 400.1 eV
Graphitic N 401.1 eV

Li et al. JACS 131, 15939 (2009)
Wang et al. ACS Nano 4, 1790 (2010)

Status and Expectation

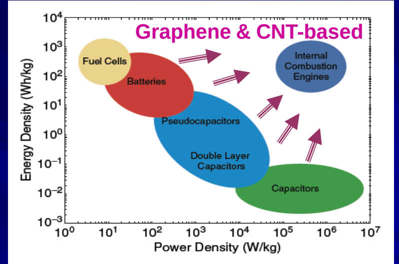

Figure 2. Comparison of the power density and energy density for batteries, capacitors, and fuel cells. (Energy is the capacity to do work; power is the rate at which work is done.)

Realization of Graphene/CNT Micro-Energy Device
Interface Physics and Chemistry

Summary (I)

- Large-scale synthesis and edge-oriented growth of multi-layer graphene (FLG, N=2-4)
- Presence of strain may be advantageous
- Superior electron transfer kinetics (ΔEp ~ 61 mV)
- On-chip direct growth of metal catalyst onto FLG shows uniform dispersion of nanoparticle (~ 3-4 nm) with enhanced forward to reverse current ratio (> 2)
- Ultra-fast (up to 1200 mV/s) charging-discharging capacitive property and high Coulomb efficiency

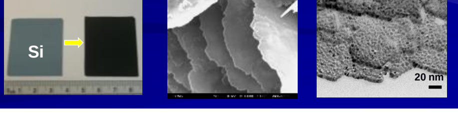

Solar to Fuel Generation

We seek as a "Holy Grail" a renewable energy source driven by solar energy that produce a clean and storable fuel….

- By Allen J. Bard and Marye Anne Fox, Acc. Chem. Res. 28 (1995) 141

- Hydrogen, the purest and zero carbon emission
- Hydrocarbons with low carbon to hydrogen ratio

Outline

- Why hydrogen economy?
- What matters?
  - Choices of materials
  - Choice of fuels or electrolytes
  - Nano enhancement
  - Surface/Interface effect

  etc. ….
- Case studies
- ZnO-, GaN-nanorods based
- Graphene oxides and hybrids

Hydrogen (Energy) Age to Come

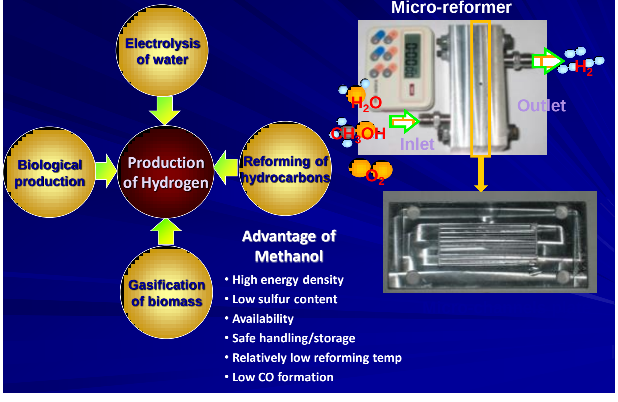

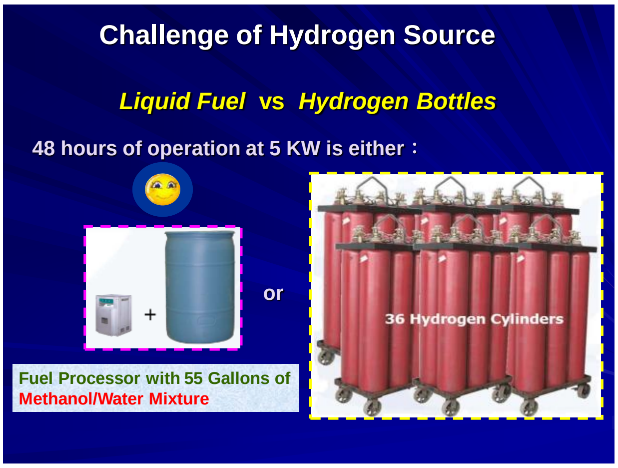
Challenge of Hydrogen Source
Liquid Fuel vs Hydrogen Bottles
48 hours of operation at 5 KW is either :
+
or
36 Hydrogen Cylinders
Fuel Processor with 55 Gallons of Methanol/Water Mixture

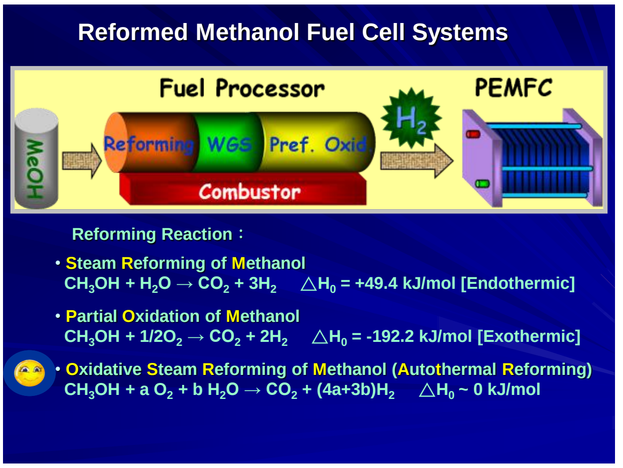
Reformed Methanol Fuel Cell Systems
Fuel Processor
PEMFC
MeOH
Reforming
WGS
Pref. Oxid
Combustor
H_2
Reforming Reaction :
• Steam Reforming of Methanol
$CH_3OH + H_2O \rightarrow CO_2 + 3H_2$ $\triangle H_0$ = +49.4 kJ/mol [Endothermic]
• Partial Oxidation of Methanol
$CH_3OH + 1/2O_2 \rightarrow CO_2 + 2H_2$ $\triangle H_0$ = -192.2 kJ/mol [Exothermic]
• Oxidative Steam Reforming of Methanol (Autothermal Reforming)
CH_3OH + a O_2 + b $H_2O \rightarrow CO_2$ + (4a+3b)H_2 $\triangle H_0$ ~ 0 kJ/mol

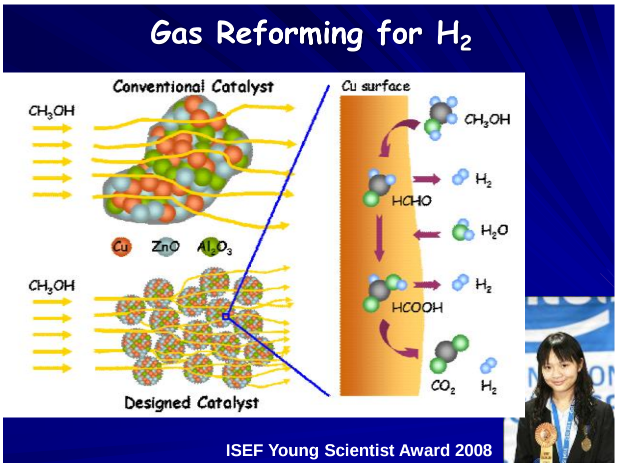
Gas Reforming for H_2
Conventional Catalyst
Cu surface
CH_3OH
Cu ZnO Al_2O_3
H_2
HCHO
H_2O
HCOOH
CO_2
Designed Catalyst
ISEF Young Scientist Award 2008

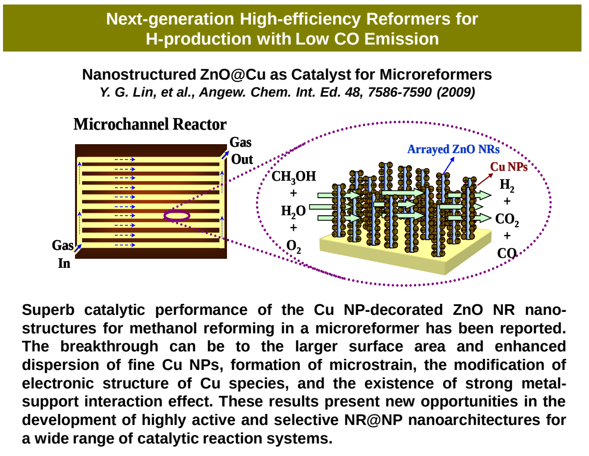
Next-generation High-efficiency Reformers for
H-production with Low CO Emission
Nanostructured ZnO@Cu as Catalyst for Microreformers
Y. G. Lin, et al., Angew. Chem. Int. Ed. 48, 7586-7590 (2009)
Microchannel Reactor
Gas Out
Gas In
Arrayed ZnO NRs
Cu NPs
CH_3OH + H_2O + O_2
H_2 + CO_2 + CO
Superb catalytic performance of the Cu NP-decorated ZnO NR nano-structures for methanol reforming in a microreformer has been reported. The breakthrough can be to the larger surface area and enhanced dispersion of fine Cu NPs, formation of microstrain, the modification of electronic structure of Cu species, and the existence of strong metal-support interaction effect. These results present new opportunities in the development of highly active and selective NR@NP nanoarchitectures for a wide range of catalytic reaction systems.

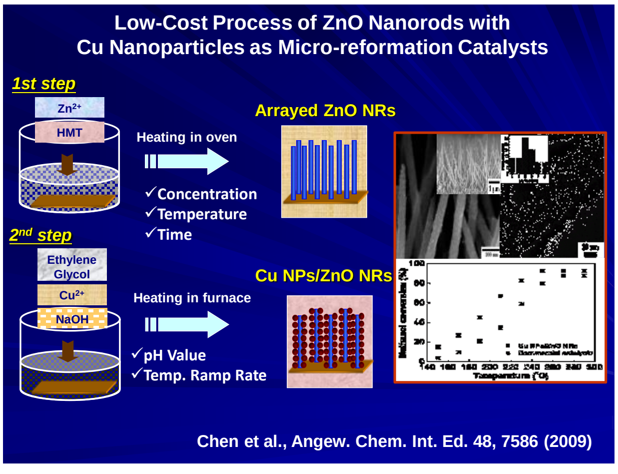
Low-Cost Process of ZnO Nanorods with
Cu Nanoparticles as Micro-reformation Catalysts
1st step
Zn^{2+}
HMT
Heating in oven
✓Concentration
✓Temperature
✓Time
Arrayed ZnO NRs
2nd step
Ethylene Glycol
Cu^{2+}
NaOH
Heating in furnace
✓pH Value
✓Temp. Ramp Rate
Cu NPs/ZnO NRs
Chen et al., Angew. Chem. Int. Ed. 48, 7586 (2009)

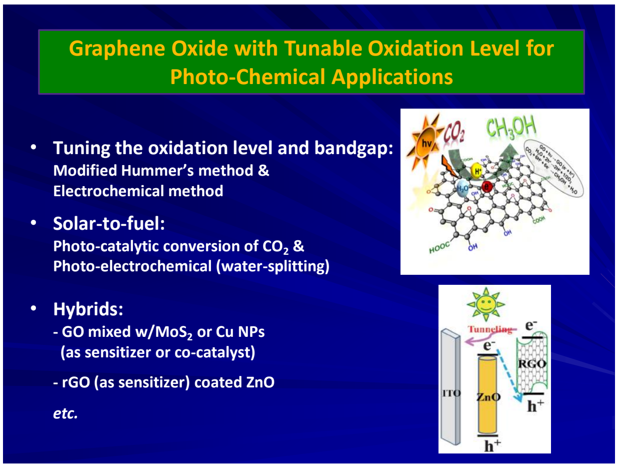
Graphene Oxide with Tunable Oxidation Level for
Photo-Chemical Applications
• Tuning the oxidation level and bandgap:
Modified Hummer's method &
Electrochemical method
• Solar-to-fuel:
Photo-catalytic conversion of CO_2 &
Photo-electrochemical (water-splitting)
• Hybrids:
- GO mixed w/MoS_2 or Cu NPs
(as sensitizer or co-catalyst)
- rGO (as sensitizer) coated ZnO
etc.
CO_2
CH_3OH
hν
Tunneling
ITO
ZnO
RGO

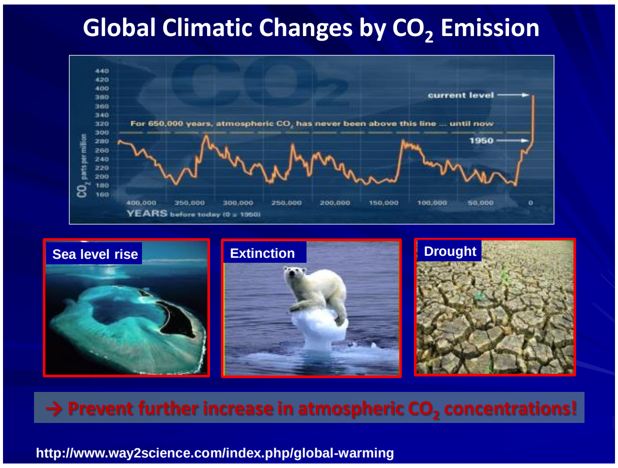
Global Climatic Changes by CO_2 Emission
current level
For 650,000 years, atmospheric CO_2 has never been above this line ... until now
1950
CO_2 parts per million
YEARS before today (0 = 1950)
Sea level rise
Extinction
Drought
→ Prevent further increase in atmospheric CO_2 concentrations!
http://www.way2science.com/index.php/global-warming

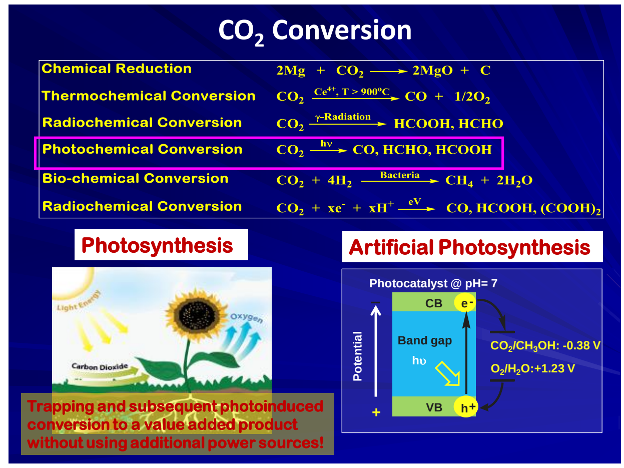
CO_2 Conversion
Chemical Reduction $2Mg + CO_2 \rightarrow 2MgO + C$
Thermochemical Conversion $CO_2 \xrightarrow{Ce^{4+}, T > 900°C} CO + 1/2O_2$
Radiochemical Conversion $CO_2 \xrightarrow{\gamma\text{-Radiation}} HCOOH, HCHO$
Photochemical Conversion $CO_2 \xrightarrow{h\nu} CO, HCHO, HCOOH$
Bio-chemical Conversion $CO_2 + 4H_2 \xrightarrow{Bacteria} CH_4 + 2H_2O$
Radiochemical Conversion $CO_2 + xe^- + xH^+ \xrightarrow{eV} CO, HCOOH, (COOH)_2$
Photosynthesis
Artificial Photosynthesis
Carbon Dioxide
Oxygen
Photocatalyst @ pH= 7
CB
Band gap
hυ
VB
Potential
CO_2/CH_3OH: -0.38 V
O_2/H_2O: +1.23 V
Trapping and subsequent photoinduced conversion to a value added product without using additional power sources!

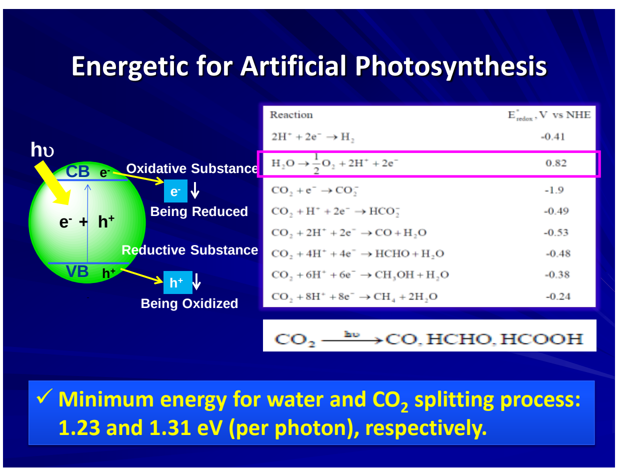
Energetic for Artificial Photosynthesis
hυ
CB
VB
Oxidative Substance
Being Reduced
Reductive Substance
Being Oxidized
Reaction E°_{redox}, V vs NHE
$2H^+ + 2e^- \rightarrow H_2$ -0.41
$H_2O \rightarrow \frac{1}{2}O_2 + 2H^+ + 2e^-$ 0.82
$CO_2 + e^- \rightarrow CO_2^-$ -1.9
$CO_2 + H^+ + 2e^- \rightarrow HCO_2^-$ -0.49
$CO_2 + 2H^+ + 2e^- \rightarrow CO + H_2O$ -0.53
$CO_2 + 4H^+ + 4e^- \rightarrow HCHO + H_2O$ -0.48
$CO_2 + 6H^+ + 6e^- \rightarrow CH_3OH + H_2O$ -0.38
$CO_2 + 8H^+ + 8e^- \rightarrow CH_4 + 2H_2O$ -0.24
$CO_2 \xrightarrow{h\nu} CO, HCHO, HCOOH$
✓ Minimum energy for water and CO_2 splitting process: 1.23 and 1.31 eV (per photon), respectively.

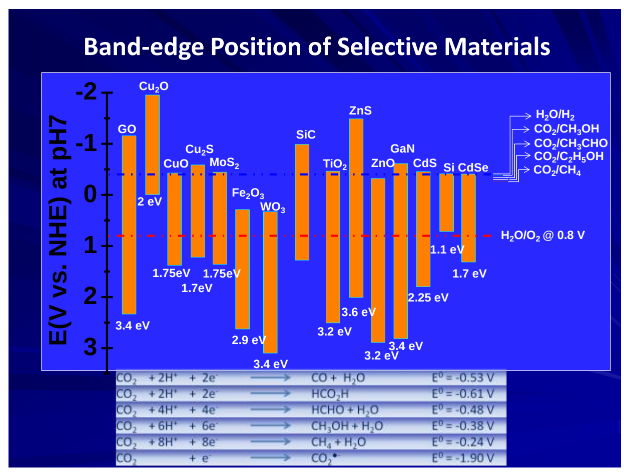
Band-edge Position of Selective Materials
E(V vs. NHE) at pH7
Cu_2O GO Cu_2S CuO MoS_2 Fe_2O_3 WO_3 SiC TiO_2 ZnS ZnO GaN CdS Si CdSe
2 eV 3.4 eV 1.75eV 1.75eV 1.7eV 2.9 eV 3.4 eV 3.2 eV 3.6 eV 3.2 eV 3.4 eV 2.25 eV 1.1 eV 1.7 eV
H_2O/H_2
CO_2/CH_3OH
CO_2/CH_3CHO
CO_2/C_2H_5OH
CO_2/CH_4
H_2O/O_2 @ 0.8 V
$CO_2 + 2H^+ + 2e^- \rightarrow CO + H_2O$ E^0 = -0.53 V
$CO_2 + 2H^+ + 2e^- \rightarrow HCO_2H$ E^0 = -0.61 V
$CO_2 + 4H^+ + 4e^- \rightarrow HCHO + H_2O$ E^0 = -0.48 V
$CO_2 + 6H^+ + 6e^- \rightarrow CH_3OH + H_2O$ E^0 = -0.38 V
$CO_2 + 8H^+ + 8e^- \rightarrow CH_4 + H_2O$ E^0 = -0.24 V
$CO_2 + e^- \rightarrow CO_2^{\bullet}$ E^0 = -1.90 V

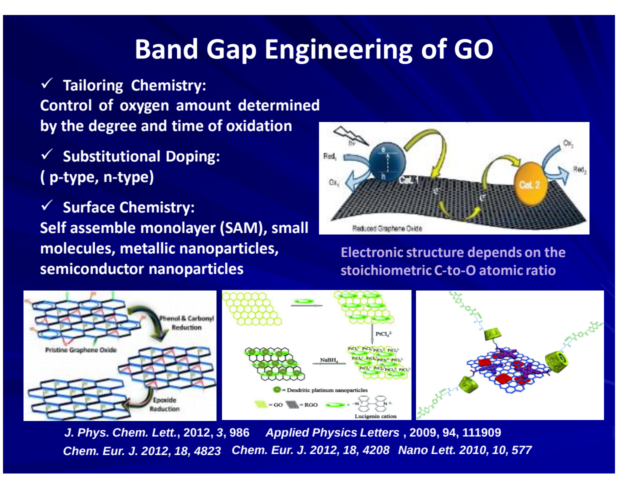
Band Gap Engineering of GO
✓ Tailoring Chemistry:
Control of oxygen amount determined by the degree and time of oxidation
✓ Substitutional Doping:
(p-type, n-type)
✓ Surface Chemistry:
Self assemble monolayer (SAM), small molecules, metallic nanoparticles, semiconductor nanoparticles
Reduced Graphene Oxide
Electronic structure depends on the stoichiometric C-to-O atomic ratio
Pristine Graphene Oxide
Phenol & Carbonyl Reduction
Epoxide Reduction
J. Phys. Chem. Lett., 2012, 3, 986 Applied Physics Letters , 2009, 94, 111909
Chem. Eur. J. 2012, 18, 4823 Chem. Eur. J. 2012, 18, 4208 Nano Lett. 2010, 10, 577

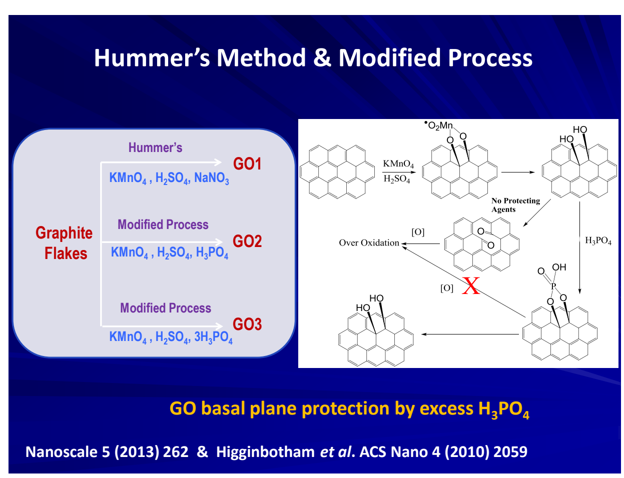
Hummer's Method & Modified Process
Graphite Flakes
Hummer's
$KMnO_4$, H_2SO_4, $NaNO_3$
GO1
Modified Process
$KMnO_4$, H_2SO_4, H_3PO_4
GO2
Modified Process
$KMnO_4$, H_2SO_4, $3H_3PO_4$
GO3
$KMnO_4$
H_2SO_4
No Protecting Agents
Over Oxidation
[O]
H_3PO_4
GO basal plane protection by excess H_3PO_4
Nanoscale 5 (2013) 262 & Higginbotham et al. ACS Nano 4 (2010) 2059

Morphology: SEM and AFM

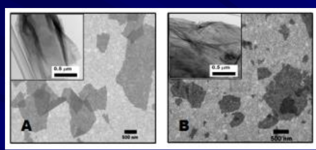

Wrinkled paper like morphology from phenolic and epoxy functional groups on the basal plane

Lateral dimensions of several micrometers and a thickness of 1-3 nm

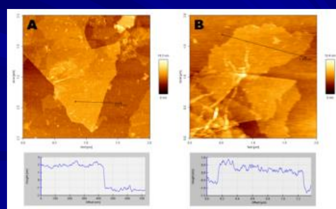

Nanoscale, 2013, 5, 262–268

Band Gap and Conduction Band Position of Graphene Oxide

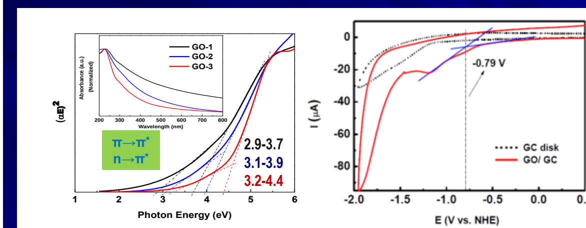

Intrinsic Semiconductor-like Absorption

CE: Pt , RE: Ag/AgCl
WE: GC
Electrolyte :0.1 M TBAP + AcCN (Sat. N_2)
Scan Rate : 100 mV s^{-1}

Nanoscale, 2013, 5, 262–268

Solar-to-Fuel Experimental Setup

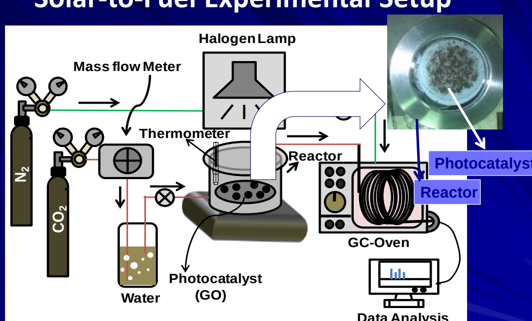

Before reaction:
1. Purging N_2 for 1h, and then CO_2 for 1h.
2. Exp. conditions:

Flow rate: 4 ml/min(Continuous flow reaction)
Light source: ELH, Reaction temperature: 30 ℃

CO_2 to Methanol Conversion

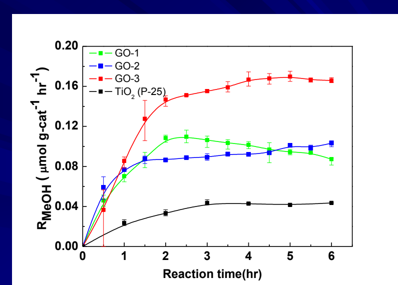

Methanol formation rate 6 times higher than TiO_2

Nanoscale, 2013, 5, 262–268

But, is this real?

Isotope Tracer Analysis:

direct evidence of the GO as effective photo-catalyst

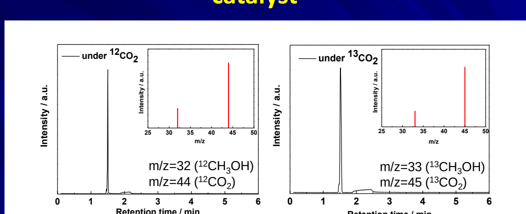

$^{12}CO_2 + 2H_2O \xrightarrow{hv} {}^{12}CH_3OH + \frac{3}{2}O_2$

$^{13}CO_2 + 2H_2O \xrightarrow{hv} {}^{13}CH_3OH + \frac{3}{2}O_2$

Nanoscale, 2013, 5, 262–268

Schematic CO_2 Reduction Mechanism on GO

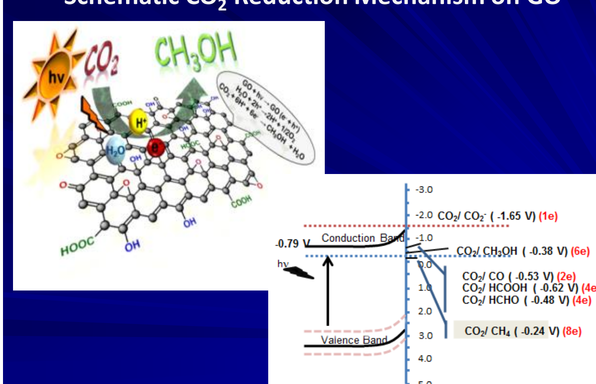

Nanoscale, 2013, 5, 262–268

Sensitizers and co-catalysts

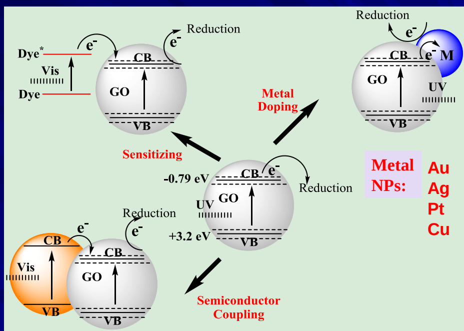

Photo-electrochemical (PEC) Process

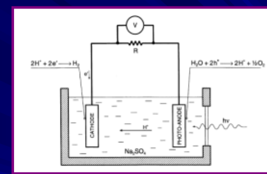

(1) Photo-generation of e-h pairs (in photo-anode)

(2) Charge separation and migration
(hole to anode-electrolyte interface &
electron to counter-electrode thru external circuit)

(3) Oxidation of water to H^+ and O_2 (at anode) &
Reduction of H^+ to H_2 (at cathode)

PEC *versus* Photocatalytic: red-ox reactions at physically separated electrode, hydrogen collected in relatively pure form, application of bias to optimize eff.

Criteria of Materials for Solar H_2 Generation

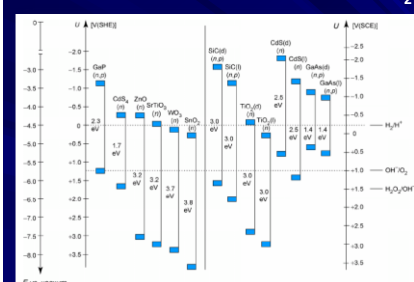

- High photon-to-electron conversion efficiency
- Band edge potentials to straddle the hydrogen & oxygen redox potentials (E_g > 1.6 eV)
- Long-term stability in aqueous solution

All must be satisfied simultaneously!

Adapted from M. Grätzel, *Nature* 414, 388 (2001)

Design rules of materials/architectures:
- Optimum light harvesting & conversion efficiency
- Compatibility with hole diffusion length

Highlights of PEC at CCMS/IAMS (I)
Solar to Hydrogen

Angew. Chem. Int. Ed. 49, 5966 (2010); J. Mater. Chem. 20, 8118 (2010); Electrochem. Comm.13, 530 (2011); Nanoscale 4, 6515 (2012); Energy & Environ. Sci. 5, 8917 (2012); Nanotechnology 24, 055401 (2013)

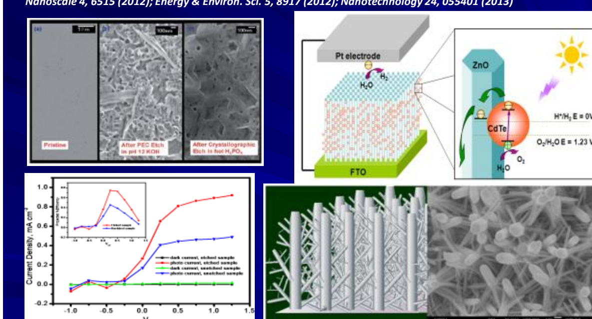

- Up to 0.98% conversion efficiency has been achieved using etched GaN.
- Up to 1.83% efficiency demonstrated using CdTe QD on ZnO NR.

Highlights of PEC at CCMS/IAMS (II)
Plasmonics Photosensitization: $Ag@Ag_3(PO_4)_{1-x}$ NPs on ZnO NRs

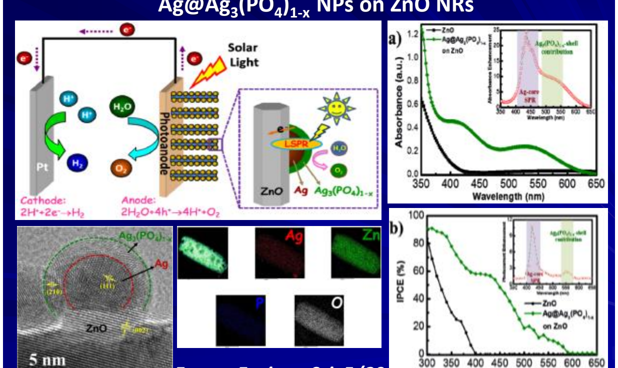

Energy Environ. Sci. 5 (201…

How about GO?
Controllable oxidation level & band gap
Tunable photo-response and photo-activity

Issues in Hummer's method:

Strong oxidation/reduction agent
High-temperature treatment
Multiple steps

Other facile, high throughput, environmental-friendly, and low cost strategy?

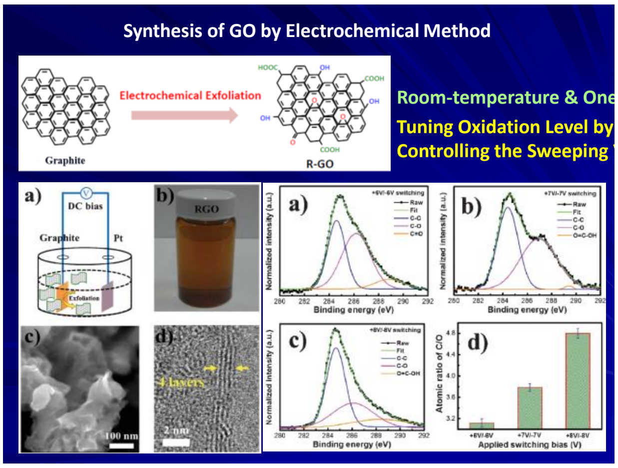

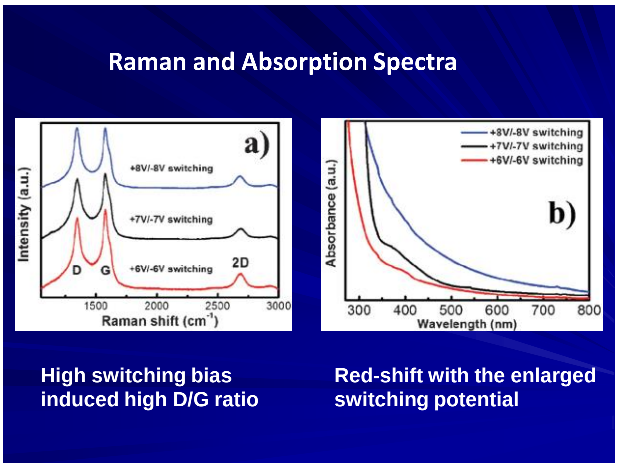

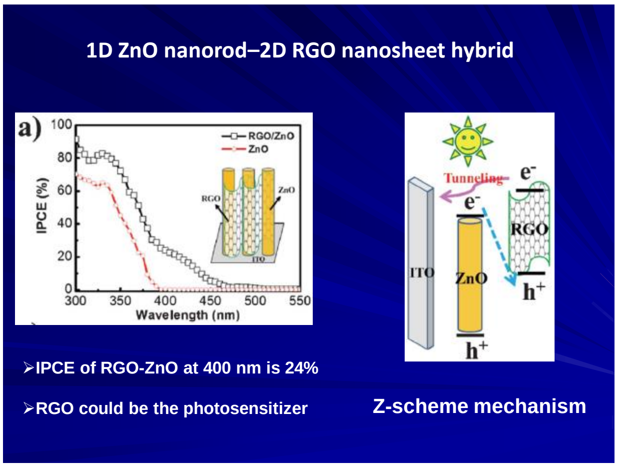

Summary (II)

- Modified GO shows good photo-catalytic activity for CO_2 reduction.
- MoS_2/GO shows solar fuel yield of 1.8 µmol g^{-1}-cat. hr^{-1} (methanol (0.8), acetaldehyde (0.25) and alcohol (0.75)).
- Cu NPs/GO shows solar fuel yield 50 times after Cu NPs modification, with methanol and acetaldehyde formation rates of 2.978 and 3.88 µmol g^{-1} cat^{-1} h^{-1}, respectively.
- GO/ZnO shows enhanced solar to hydrogen efficiency.
- Controllable oxidation level and band gap of GO is demonstrated by one-step, room-temp. EC method.